Evolution of resistance to COVID-19 vaccination with dynamic social distancing

How does open access to this work benefit you?
Let us know @ library@weizmann.ac.il

Take down policy
The Weizmann Institute of Science has made every reasonable effort to ensure that Weizmann Institute of Science content complies with copyright restrictions. If you believe that the public display of this file breaches copyright please contact library@weizmann.ac.il providing details, and we will remove access to the work immediately and investigate your claim.

(article begins on next page)

Evolution of resistance to COVID-19 vaccination with dynamic lockdown

Gabriela Lobinska*[1], Ady Pauzner[2], Arne Traulsen[3], Yitzhak Pilpel*[1], Martin A Nowak*[4]

1 Department of Molecular Genetics, Weizmann Institute of Science, Rehovot 76100, Israel

2 Berglas School of Economics, Tel Aviv University, Tel Aviv 69978, Israel

3 Department of Evolutionary Theory, Max-Planck-Institute for Evolutionary Biology, August-Thienemann-Str. 2, 24306 Ploen, Germany

4 Department of Mathematics, Department of Organismic and Evolutionary Biology, Harvard University, Cambridge MA 02138, USA

The COVID-19 pandemic has led to an unprecedented global response in terms of social lockdown in order to slow the spread of the virus [1], [2]. Currently the greatest hope is based on world-wide vaccination[3], [4]. The expectation is that social and economic activities can gradually resume as more and more people become vaccinated. Yet, a relaxation of social distancing that allows increased transmissibility, coupled with selection pressure due to vaccination, will likely lead to the emergence of vaccine resistance [5]. Here we analyze the evolutionary dynamics of COVID-19 in the presence of dynamic lockdown and in response to vaccination. We use infection and vaccination data of 6 different countries (Brazil, France, Germany, Israel, UK, US) [2]. For slow vaccination rates, resistant mutants will appear even if strict lockdown is maintained. For fast vaccination rates (such as those used in Israel) the emergence of mutants can be prevented if strict lockdown is maintained during vaccination. We analyze multiple human factors that affect the evolutionary potential of the virus, including the extent of dynamic lockdown, vaccination campaigns, boosters and vaccine hesitancy. The emergence of vaccine resistance can also be prevented by developing two-gene vaccines. Our results provide guidelines for policies that aim to minimize the probability of emergence of vaccine resistance variants.

The COVID-19 pandemic has had a devastating effect on global health and economy. Since the identification of the first SARS-COV-2 case in December 2019, 178.71 million infections have been recorded and at least 3.86 million people have died as a result of the infection (as of June 2021)[2]. The increased mortality and complication rates of SARS-COV-2[1] compared to the mild diseases caused by seasonal coronaviruses, such as HCoV-229E[6], have led to unparalleled governmental and individual-level responses in order to reduce the number of SARS-COV-2 infections.

Since the beginning of the pandemic, it has become clear that many of the non-pharmaceutical interventions (NPI), such as lockdowns, are economically and socially unsustainable in the long run. Periodical loosening and tightening of social distancing measures, which present an attempt at balancing economical and sanitary considerations, have led to waves of increase and decrease in the number of SARS-COV-2 infections per day[2] (see **Figure 1A**). Therefore, much hope has been placed on vaccine development, which would allow the immunization of a large fraction of the population, thereby substantially reducing mortality and potentially achieving herd immunity, which could in principle eradicate SARS-COV-2 altogether.

Mass vaccination campaigns have been launched in many countries (see **Figure 1B**), most notably Israel and the UK (both more than 60% of fully vaccinated population) and the US and Germany (both more than 50% of fully vaccinated population). Currently, four companies are producing vaccines that have been approved for emergency use either by the Food and Drug Administration (FDA)[3] or by the European Medicines Agency (EMA)[4]: Pfizer-Biontech, Moderna, AstraZeneca and Johnson & Johnson/Janssen Pharmaceuticals. Several other vaccines are also used outside of the European Union and the USA: Gamaleya (Sputnik V), Sinopharm Beijing, Sinovac, Sinopharm-Wuhan and Bharat-Biotech (Covaxin)[7].

However, the identification of new SARS-COV-2 variants has cast a shadow over the expectation of a swift end of the pandemic[8], [9]. The so-called "British" variant (B.1.1.7), now termed α, and "South African" variant (501.V2), now termed β, have been shown to be neutralized to a lesser extent by convalescent and vaccinee sera[10], although experiments on non-human primates have shown that this decrease might not necessarily cause a decrease in immunity[11]. Structural studies have mapped and predicted mutations that lead to antibody escape[12]–[14]. As vaccination around the world progresses, the continued evolution of SARS-COV-2 could eventually give rise to a fully vaccine resistant variant. Such a variant could quickly spread due to its ability to infect vaccinated and recovered in addition to fully susceptible individuals. The question of emergence of vaccine resistance has already been the subject of many research papers[15]–[18].

What policy could be exercised that would minimize the chance of emergence of vaccine resistant strains? Policymakers can vary the extent of social distancing imposed and regimes of vaccine administration. The critical biological parameters on the other hand include the infectivity of the various strains and the rate of mutation of the virus that may ultimately lead to emergence of a resistant strain. Here we introduce a mathematical model that examines various combinations of these parameters. Our model helps to design optimal policies that would minimize the chance of emergence of resistant strains or maximize the time until their occurrence.

Our paper is an addition to the extensive body of work that has been performed in the past year in order to understand the spread and evolution of SARS-COV-2[19]–[25]. SARS-COV-2 research has drawn on a very long

63 history of epidemiological research[26], [27], [36]–[38], [28]–[35]. Due to the global and urgent nature of the

64 pandemic, many studies that could inform policy-making have been conducted[5], [39], [48], [40]–[47].

65 In order to understand the evolutionary potential of the virus in response to a vaccination program we study a

66 stochastic model for infection dynamics and virus evolution in the presence of varying degrees of social

67 lockdown and different vaccination rates. We distinguish between a wild-type virus (WT) and a vaccine resistant

68 mutant virus (MT). The vaccine is effective against the WT strain, while the MT strain evades immunity induced

69 by the vaccine either partially or completely. We build upon the mathematical framework of the Susceptible-

70 Infected-Removed (SIR) model from epidemiology [32], [49], albeit with considerable adjustments necessitated

71 by the specific problem at hand . Our model keeps track of people who are susceptible, infected by WT or MT,

72 recovered from WT or MT, vaccinated or unvaccinated (**Figure 2**).

73 Crucially, we assume there is a dynamic lockdown guided by the number of new infections per day. As that

74 number exceeds a threshold, governmental rules and individual responses reduce social activity. If the number

75 of new infections falls below this threshold, the lockdown is somewhat relaxed and some people stop following

76 the rules, thereby allowing higher transmission of the virus. We simulate these dynamics as a stochastic process.

77 In consequence, we obtain fluctuating numbers of new infections per day. We introduce mass vaccination at

78 alternative fixed rates. Then we compute the probability and timing of the wave of infection caused by the

79 spontaneous emergence of a vaccine resistant virus.

80 In our approach, the mutation rate μ denotes the probability that a WT-infected individual will infect a

81 susceptible individual with the MT strain. The exact value of this probability is currently unknown and complex

82 to obtain empirically. For the simulations and calculations reported in this paper we therefore consider a wide

83 range of mutation rates. From our model, we also derive an upper bound for the mutation rate using the fact

84 that no wave of a vaccine-resistant variant has occurred up until now. Note that this rate can be very different

85 from the per-base mutation rate of SARS-COV-2, which is about 10^{-5}.

86

87 DYNAMICS OF VIRAL INFECTION AND EVOLUTION

88 Our model keeps track of eight different variable states: individuals who are susceptible (x), infected with WT

89 (y_1), non-vaccinated and infected with MT (y_{2A}), vaccinated and infected with MT (y_{2B}), recovered from WT

90 (z_1), recovered from MT (z_2), vaccinated but susceptible to MT (w_1), vaccinated and recovered from MT (w_2);

91 see **Figure 2**.

92 The WT strain can infect susceptible individuals (x), converting them to individuals infected with WT (y_1) at rate

93 β_1. A mutation can occur with probability μ. In this case, a WT infected individual infects a susceptible individual

94 (x) with a mutated version of the virus, in a mutation that have taken place in the infecting individual, thus

95 converting the susceptible to a MT infected individual (y_{2A}). WT infected individuals either recover with rate a

96 and become immune to future WT infection (z_1) or die at rate d. Susceptible individuals (x) and individuals

97 recovered from WT (z_1) can become vaccinated individuals (w_1). The parameter c denotes the number of

98 individuals vaccinated per day. Hence, the rates of vaccination of x, z_1 and z_2 are respectively $cx/(x + z_1 + z_2)$,

99 $cz_1/(x + z_1 + z_2)$ and $cz_2/(x + z_1 + z_2)$. For simplicity we assume single-dose vaccination; for a double dose

100 vaccine our model would describe the application of the second dose ignoring partial immunity caused by the

101 first dose; extension of our model to a full two dose vaccination protocol is straightforward. Although several

102 countries display a logistic-shaped vaccine distribution curve, we show that the above linear assumption does

103 not significantly affect the probability of emergence of vaccine resistance (see **Supplementary Figures S1** and

104 **S2**).

105 At rate β_2, the MT strain infects susceptible individuals (x), WT recovered individuals (z_1) and vaccinated

106 individuals who are not immune to MT (w_1). MT infected individuals either recover with rate a and become

107 immune to future MT and WT infection (z_2) or die at same death rate d as with the WT strain, i.e. assuming no

108 difference in lethality between the two strains. While we consider death due to infection, the focus of this paper

109 is not to model the number of deaths, nor public health metrics such as ICU usage or available respirators. We

110 assume one-way cross-immunity induced by the viral strains: the MT strain can infect individuals that have

111 recovered from WT or that have been vaccinated against WT, but the WT strain cannot infect individuals that

112 have recovered from the MT. This assumption is reasonable because the MT evolves in the presence of the WT,

113 but not vice versa. We note that our MT strain escapes both from the immunity that is induced by natural

114 infection with WT and the immunity induced by vaccination against WT. We assume that the partial immunity

115 to the vaccine resistant variant induced by infection with wild type is equal to that induced by vaccination. A

116 recent study suggests that individuals that are both recovered and vaccinated benefit from higher immunity

117 than only vaccinated individuals. In the Supplementary Materials (**Figures S3** and **S4**) we study this effect.

118 We need to distinguish between MT infected individuals that are or are not vaccinated: y_{2B} and y_{2A},

119 respectively. Upon recovery the former will not be vaccinated (again), while the latter will be vaccinated.

120 We also study partial immunity to the MT strain which can be acquired by recovery from WT infection or by

121 vaccination. For partial immunity, the corresponding infection rates are multiplied by a parameter q, which is

122 between 0 and 1. If $q = 1$ then WT infection or vaccination confers no immunity to MT at all; the mutant escapes

123 completely. For $0 < q < 1$, the MT is a partial escape mutant. For $q = 0$, the MT does not escape at all.

124 Lockdown measures are implemented by multiplying the infectivity coefficients of each strain by a social activity

125 parameter s which ranges in $[0,1]$. Unconstrained social interaction means $s = 1$, while $s = 0$ would be

126 complete lockdown. The population tolerates a certain number of new infections, L, per day. Each day, if the

127 number of new infections exceeds L, then s is decreased by a random, uniformly distributed number between

128 0 and 0.1, noted s_0. If the number of new infections is less than L, then s is increased by a random, uniformly

129 distributed number between 0 and 0.1. In any case, s cannot decrease below 0.05 or increase above 1. In our

130 simulations, we adjust the parameter s every day. We then obtain a near constant number of cases per day. In

131 Supplementary Materials, we explore less frequent adjustments of the parameter (such as every week) and

132 conclude that our results are robust (see **Figure S5** and **Figure S6**.) Our social activity parameter s can be

133 interpreted to include other factors that could potentially affect transmissibility, such as seasonality. In

134 Supplementary Materials (see **Figure S7** and **Figure S6**), we explore the effect of seasonality.

135 As an example, the rate of infection of the recovered from WT z_1 by the MT strain infected individuals y_2 is

136 multiplied both by the lockdown coefficient s and the partial immunity coefficient q – hence this rate is given

137 by $q\beta_2 s w_1 y_2$.

138 All model parameters are summarized in **Table 1.**

139 COMPUTATIONAL IMPLEMENTATION AND DATA

140 A Gillespie algorithm is commonly used to simulate stochastic systems with high variation in waiting times

141 between consecutive events [50]–[53]. In our model the population is represented as a vector of length eight,

142 corresponding to the eight categories. The rates of all possible events (infection, recovery, death, mutation and

143 vaccination) are calculated. The time of the next event in the model is drawn from an exponential distribution,

144 with parameter dependent on the sum of all event rates and an event is chosen, with probability proportional

145 to its rate. The population is updated according to the event that occurred. The simulation is stopped when

146 there are no more infected individuals in the population. The algorithm is presented in pseudocode in the

147 **Appendix**, along with a table of the possible events of the model and their default rates.

148 In order to achieve feasible computation time and resources, we simulated populations of size up to $N = 10^6$.

149 The results of those simulations can be scaled to larger population sizes by considering a population of for

150 example $N = 10^7$ as $m = 10$ "batches" of 10^6 individuals, and computing the results for $N = 10^7$ as

151 $1 - (1 - p)^m$, where p is the proportion of runs where the MT strain took over. **Figure S8** shows the strong

152 agreement between simulated results and the results scaled from simulations with smaller population sizes.

153   For all our simulations, we have endeavored to use real world data for all model parameters. In particular,

154   infection and vaccination data has been obtained from the database *Our World in Data* [2] (OWID) and

155   downloaded on June 19th, 2021.

156   In our simulation, since the number of new infections each day is constant, the number of susceptible individuals

157   decreases linearly with slope $-L/a$. Vaccination of both susceptible and recovered individuals proceeds at rate

158   c. The social activity parameter, s, increases as more and more individuals become immunized either by

159   infection or by vaccination. The WT reproductive rate, R_{WT} , is maintained at 1 as long as the MT has not

160   appeared. The MT reproductive rate, R_{MT} , increases with the social activity parameter s until the MT strain

161   takes over. After MT takeover, the MT reproductive rate R_{MT} is buffered at 1 by the dynamic lockdown (see

162   **Figure 3** and **Methods**).

163   We performed 1000 runs of the stochastic simulation for each combination of parameters reflecting realistic

164   values of the two model parameters determined by governmental policy: the tolerated number of infections

165   per day, L, and the vaccination rate per day, c. Each square of the color map shown in **Figure 4** reflects the

166   average value of these 1000 runs, which were performed for a population of $N = 10^6$ and then scaled to $N =$

167   10^7 and $N = 10^8$. At each combination of L and c the color maps denote the predicted probability of a mutant

168   take over. We perform computations using $q = 1$ and $q = 0.4$ for complete and partial immune evasion by the

169   mutant.

170   Allowing a large amount of infection cases and slow vaccination results in almost certain takeover of the MT

171   strain. On the other hand, very fast vaccination coupled with a low number of tolerated new infections per day

172   can prevent emergence of the MT. Partial immune evasion $(q = 0.4)$ of the mutant slightly reduces the

173   probability of its takeover. Note that the shape of the parameter space where we observe takeover is similar

174   for $q = 1$ and $q = 0.4$.

175   Although estimating COVID-19 mortality is not the focus of this paper, we have also recorded the number of

176   deaths in the first 365 days of the simulation. The results are shown in **Figure S9** of the Supplementary Materials.

177   REPRODUCTIVE RATIO OF THE MUTANT AND PROBABILITY OF TAKEOVER

178   In **Figure 5** we show detailed data from 6 countries together with the estimated reproductive ratio, R_{MT}, of a

179   vaccine resistant mutant and the probability of generating a wave of resistant virus. Data for the number of

180   susceptible individuals $x(t)$, vaccinated individuals $w(t)$, recovered individuals $z(t)$, newly infected individuals

181     $L(t)$, and an estimate for the reproductive rate R_{WT} of the WT can be obtained from *OWID* [2]. The reproductive

182   rate R_{MT} of the escape mutant can be calculated according to:

$$R_{MT}(t) = R_{WT}(t)[x(t) + qw(t) + qz(t)]/x(t) \qquad (1)$$

183 The probability of not producing an escape mutant in a given day is $(1 - \mu)^{L(t)}$. The probability of not

184 producing a surviving escape mutant is $(1 - \rho(t)\mu)^{L(t)}$, where $\rho(t)$ is the survival probability of a mutant

185 generated on that day. If $R_{MT}(t) < 1$ then $\rho(t) = 0$. If $R_{MT}(t) > 1$ we assume $\rho(t) = 1 - 1/R_{MT}(t)$. The

186 probability that no surviving mutant is generated between time 0 and time t is given by

$$P(t) = \prod_{\tau=0}^{t}[1 - \mu\rho(\tau)]^{L(\tau)} \qquad (2)$$

187 In **Figure 5** we show the reproductive rate of the mutant $R_{MT}(t)$ and the probability $P(t)$ of generating a

188 surviving escape mutant as a function of time. Prior to vaccination the reproductive rate of a potential escape

189 mutant tracks closely that of the WT. As people become vaccinated in large numbers, R_{MT} starts to increase

190 significantly above R_{WT}. Nevertheless, it is possible to keep R_{MT} below one by maintaining some measures of

191 lockdown. (This is the case for Israel and UK). Overall, the probability that Israel generated a vaccine escape

192 mutant (before June 2021) is of order of 1-2 percent (assuming $\mu = 10^{-7}$). For the same mutation rate the

193 corresponding probability for the United States is 32 percent; the United States have a much larger total

194 population size but also many more infections per million people. The corresponding probabilities for Brazil,

195 France, Germany, and UK are 17, 8, 4 and 6 percent (see **Table 2**).

196 ESTIMATING THE MUTATION RATE μ

197 We suggest a method to estimate an upper bound of the mutation rate μ from WT to MT based on the

198 observation that despite a large number of infections since the beginning of the pandemic and including recent

199 vaccination campaigns, no immune evasive mutant has yet taken over. Our method for calculating an upper

200 bound of the mutation rate is potentially applicable for estimating any mutation rate between two phenotypes

201 in an evolving population. The upper bound is computed at any given time point, and can be updated and

202 become tighter if in future an evasive strain still does not appear.

203 Let us assume that the real value of the mutation rate equals μ^*. For each country, we have an estimate of the

204 reproductive coefficient of the MT strain and the number of new infection cases for each day (see **Figure 5**) for

205 each day from the beginning of the pandemic until August 15th, 2021. Hence, we can calculate the probability

206 that the MT strain would have emerged by August 15th, 2021 assuming a mutation rate μ^*. If this probability is

207 higher than 0.5, then the probability that the MT strain would have been observed on August 15th, 2021 is higher

208 than not, given that the mutation rate equals μ^*. Since as of August 15th, 2021, an MT strain has not been

209 observed, then our estimate of the mutation rate must be lower than μ^*. We define the upper bound for the

210   mutation rate on a given day as the value μ for which the probability that the MT strain would have taken over

211   by that day is 0.5.

212   Hence, for each day, we compute the probability that the MT strain would have taken over until that day given

213   a mutation rate using Eq. (2). We assume $q = 1$, which means the MT strain is fully immune evasive. The

214   resulting function for probability of mutant take over (for a given time point) versus mutation rate has a

215   sigmoidal shape, with its midpoint corresponding to the mutation rate for which it is equally probable that the

216   MT strain would have taken over or not, i.e. our definition for the upper bound of the mutation rate. In **Figure**

217   **6A**, we show the probability of emergence of the MT strain on July 30th, 2020 given data from the six considered

218   countries. The upper bound estimate for the United States is the x-axis value for the point indicated by the red

219   arrow, i.e. the midpoint of the sigmoidal function. The probability of emergence of the MT strain until August

220   15th, 2021 for a given mutation rate is higher than it was on July 30th, 2020 since many infections have occurred

221   since then. Hence, the upper bound estimate for the United States has decreased, i.e. shifted to the left on the

222   x-axis (see position of the red arrow) (see **Figure 6B**).

223   Therefore, the estimated upper bound on the mutation rate decreases over time as long as more infections do

224   not give rise to a MT strain (see **Figure 6C**).

225   Since the probability of MT takeover (Eq. (2)) is strongly dependent on the number of infections, significant

226   decreases in the estimated values correspond to periods with high infection rates in which, nonetheless, a

227   mutant did not appear. The estimate for the upper bound of the mutation rate is expected to plateau as

228   vaccination campaigns lead to a decrease in the number of infection cases. The estimate of 10^{-6} will decrease

229   further if and when large countries such as the US will advance in the vaccination campaign with no mutant

230   takeover. Using the world infection and vaccination data, we obtain $\mu = 10^{-7}$ as the order of magnitude for the

231   upper bound for the rate at which immune evasive mutants appear. But estimates based on individual countries

232   may be more informative since the world data reflects the average over an extremely heterogeneous population

233   subject to very different policies.

234   Can we estimate a lower bound for the mutation rate? Our method could be potentially applicable for

235   estimating the lower mutation rate, assuming that a vaccine resistant has emerged. Then, we could compute

236   the value of μ given the date of emergence and assuming that the probability of emergence on that day has

237   become higher than 0.5. Let us assume that an MT strain did takeover on August 15th, 2021. Then, numerically

238   solving Eq. (2) plugging in data from the United States yields $\mu = 2.2 \cdot 10^{-7}$ (which is also the upper bound,

239   assuming that the MT strain has not taken over).

A SIMPLE FORMULA FOR THE ESCAPE PROBABILITY

240

241   The dynamic lockdown captured by the social activity parameter $s(t)$ maintains the number of new infections

242   per day fluctuating around a fixed value and thereby buffers the reproductive ratio of the wildtype R_{WT} around

243   1. The number of active infections is roughly constant and given by L/a, where a is the recovery rate (see **Figure**

244   **3**). If vaccination is slow, $c \ll L$, then the change in the number of susceptible, $x(t)$, and recovered individuals,

245    $z_1(t)$, over time can be described by linear functions with slopes proportional to L (see **Methods and Figure**

246   **S10A**).

247   Alternatively, for fast vaccination, $c \gg L$, the change in the number of susceptible $x(t)$ and vaccinated

248   individuals $w_1(t)$ can be described by linear functions with slopes proportional to c before MT takeover, and

249   with slopes proportional to L after MT takeover (see **Methods and Figure 3E**). Neglecting vaccination of

250   recovered individuals (which is a reasonable approximation for $c \gg L$) we can write $(t) = N - Lt - ct$, $z(t) =$

251   Lt and $w(t) = ct$. The time when herd immunity against the WT is reached is given by

$$T_H = \frac{N}{c + L} \left(1 - \frac{1}{R_0}\right) \tag{3}$$

252   During vaccination the reproductive rate of the mutant increases as (see **Methods**)

$$R_{MT}(t) = \frac{N}{N - (L + c)t} \tag{4}$$

253   The reproductive rate of the MT is initially 1 and increases to R_0 as people recover from WT infection or are

254   vaccinated (see **Figure 3D**). Once a mutant has been generated, the probability of its survival depends on the

255   value of the reproductive rate, $R_{MT}(t)$. The probability that no surviving mutant has appeared before time t,

256   where $t \leq T_H$, can be calculated to be (see **Methods**):

$$P(t) = \exp[-\left(\frac{\mu N}{2}\right)\left(\frac{L}{N}\right)\left(\frac{c + L}{N}\right)t^2] \tag{5}$$

257   The probability that no surviving mutant has appeared until herd immunity is

$$P(T_H) = \exp\left[-\left(\frac{\mu N}{2}\right)\left(\frac{L}{c + L}\right)\left(1 - \frac{1}{R_0}\right)^2\right] \tag{6}$$

258   Here $R_0 = \beta N/a$ is the basic reproductive ratio of the WT. The corresponding formulas for partial immune

259   escape mutants are given in the **Methods**. Eq. (6) is in good agreement with the results of exact stochastic

260   simulations (**Figure S11**). In addition, we derive $P(T_H)$ for more infectious mutants, i.e. $\beta_2 > \beta_1$ (see **Methods,**

261   and **Figure S12**). We also explore simulation results for mutants that are less infectious than the wild type in the

262   Supplementary Materials (see **Figure S13**). We notice that the probability $P(T_H)$ does not depend on parameters

263   β, a, s_{thres} and d. In order to confirm that the value of these parameters does not affect the probability of

264   emergence of a vaccine resistant variant, we have included a sensitivity analysis in the Supplementary Materials

265   (see **Figure S14**).

266   In **Table 3**, we show how the probability and timing of resistance depends on the vaccination rate and the

267   number of new infections per day. We first consider a large country of $N = 10^8$ inhabitants and a mutation rate

268   of $\mu = 10^{-7}$. If 10,000 new infections occur per day and 1 million people are vaccinated per day, then herd

269   immunity is reached in 66 days and the probability of generating a vaccine resistant mutant is about 2 percent.

270   For the same vaccination rate, if 50,000 new infections are tolerated each day, then the probability of generating

271   an escape mutant increases to 10 percent. If 10,000 new infections occur per day but only 100,000 people are

272   vaccinated every day, then the probability of generating vaccine resistance increases to 18 percent.

273   As the proportion of vaccinated individuals grows, social distancing measures relax, and the probability of

274   emergence of resistance increases. Hence, higher vaccination rates are associated with higher probabilities of

275   resistance after 50, 100 and 200 days (see **Table 2**). However, faster vaccination leads to earlier herd immunity.

276   When herd immunity is reached, there are no more new infections and the cumulative probability of resistance

277   plateaus. Therefore, we observe an interesting counterintuitive effect: the probability of resistance until a fixed

278   time t increases with the vaccination rate c, but the probability of resistance until time T_H when herd immunity

279   is achieved decreases with the vaccination rate c. (see **Table 3 and Figure S15**).

280   We can derive estimates for the emergence of vaccine resistant strains using current vaccination and infection

281   rates from around the world. If the whole world ($N = 8 \cdot 10^9$) vaccinated as fast as the US ($c = 5000$ per day

282   per million) and had slightly lower infection rates than Germany ($L = 100$ per day per million) then herd

283   immunity would be achieved in $T_H = 131$ days; the probability that a resistant virus was generated and survived

284   by that time would be 0.97 (for $\mu = 10^{-7}$) and 0.29 (for $\mu = 10^{-8}$). If the whole world vaccinated as fast as

285   Brazil ($c = 3000$ per day per million) and had infection rates like the US ($L = 250$ per day per million) then

286   herd immunity would be achieved in $T_H = 205$ days; the probability that a resistant virus was generated and

287   survived by that time would be 0.999 (for $\mu = 10^{-7}$) and 0.75 (for $\mu = 10^{-8}$). Our results underline the

288   importance of maintaining lockdown measures while herd immunity is not achieved and timely distribution of

289   vaccines around the world.

290

291

PREVENTING EMERGENCE OF VACCINE RESISTANCE

Improved vaccine design

The probability of emergence of vaccine resistance can be reduced by increasing the number of vaccinated people per day (c) and reducing the number of allowed infections per day (L) until herd immunity is reached.

However, policymakers could also affect the mutation rate μ by determining what type of vaccine is used. We have extended our basic model to consider vaccine resistance achieved when two independent mutations are present (see **Figure S16** and **Figure S17**). Each mutation is neutral by itself. We find that for realistic mutation rates, that is mutation rates below our estimated upper bound, vaccine resistance never emerges when two-gene vaccines are distributed (see **Figure S18**). This extension can also be interpreted as the case where two independent mutations are needed to confer resistance to a vaccine based on a single gene. But using two mRNAs in a single vaccine could double the number of mutations needed to achieve immune escape.

Reducing vaccine hesitancy

In most developed countries, vaccine hesitancy has caused the number of vaccinated individuals to plateau. Vaccine hesitancy can also be reduced by policy decisions. In **Figure S19** and **S20**, we extend our model to account for the proportion of population that will not be vaccinated. We find that although high vaccine hesitancy substantially increases the probability of emergence of vaccine resistance, low vaccine hesitancy can actually have a negligible effect. For $R_0 = 3$, the levels of vaccine hesitancy necessary to significantly increase the probability of emergence of vaccine resistance are much higher than the vaccination hesitancy rates in many of the considered countries except for Brazil and the United States. However, more infectious mutants have emerged in the past months.

In order to achieve herd immunity, a certain fraction of the population must become immunized to the infecting agent. Immunization can either occur by recovery from infection or by vaccination. The minimum fraction of immunized required for herd immunity increases with the reproductive coefficient R. If a certain proportion of the population will not be vaccinated, then an excess of infections will occur in order to achieve the proportion of immunized required for herd immunity. This excess of infections increases the probability of emergence of vaccine resistance. For $R_0 = 3$, the fraction of immunized required for herd immunity is 2/3. Hence, 1/3 of the population can remain susceptible without affecting the probability of emergence of a vaccine resistance variant. However, with more infectious variants, this tolerated proportion of non-vaccinated is lower. For

example, for R = 5, the proportion of non-vaccinated such that the probability of vaccine emergence is unchanged is only 20%. As vaccination is expected to be extended to more age groups, the proportion of unvaccinated individuals could further decrease until vaccine hesitancy ceases to be a concern for emergence of vaccine resistance.

In most countries, vaccine hesitancy seems to be a function of age. Hence, we can estimate the expected vaccine hesitancy given the age structure of each of the six considered countries. Many countries have still not experienced a plateau in the total number of vaccinated for their younger population. The exception could be Israel. In Israel, 80.2% of the 20-29 year olds are vaccinated. In France, only about 50% of that age group is vaccinated, and the number of new vaccinations per day has not yet reached a plateau. We expect that many of the 20-29 year olds in France will still become vaccinated, thus increasing the total number of vaccinated people in the population.

Using boosters to counteract waning of immunity

The waning of immunity has recently become a concern. We have extended our model to consider waning of immunity after 180 days after vaccination or recovery (see **Figure S21** and **Figure S22**). When no booster vaccination is administered, the probability of emergence of vaccine resistance does increase substantially, especially for high vaccination rates. However, a booster vaccination campaign conducted after 180 days can reduce the probability of emergence of vaccine resistance back to basic model levels (see **Figure S23**).

SUMMARY

We have studied evolution of resistance to COVID-19 vaccination in the presence of dynamic lockdown. We use real world data to simulate the spread of the SARS-COV-2 virus. We have performed stochastic simulations and obtained analytical results. In particular, we have derived a simple intuitive formula for the probability of emergence of a vaccine resistant strain over time (Eqs. (5) and (6)).

Our basic model makes a series of simplifying assumptions, including: (i) no seasonality of the infection patterns; (ii) vaccination of the whole population; (iii) no waning of immunity; (iv) linear distribution of vaccine doses and (v) rapid social response to rising infection numbers. We have studied model extensions that remove those simplifications (see **Supplementary Materials Figures S1-S7, S12-S13, S16-S23**). We have assumed a stochastic model – this is because the appearance of a vaccine resistant strain, and in particular its non-extinction due to random drift, is by nature stochastic.

354   Our model most closely corresponds to the assumption that immune evasion could be due to a single point

355   mutation. Nevertheless, our estimates of the mutation rate between the wild-type and immune evasive strains

356   could signify that a combination of mutations is needed to achieve immune evasion. Therefore, we have

357   explored lower effective mutation rates than the current estimation for the per-base mutation rate of the SARS-

358   COV-2 virus.

359   The probability of takeover of an immune evasive strain is mostly dependent on the number of total infection

360   cases that occur during the pandemic. Social distancing measures, such as lockdowns, can delay or event prevent

361   the emergence of the MT strain. Each natural infection is an opportunity for the MT strain to appear and possibly

362   take over. Hence, the main policy goal should be to maximize the proportion of the population which will be

363   immunized to the virus through vaccination as opposed to natural infection.

364   In terms of policy implications, our result supports the maintenance of social distancing measures until the daily

365   number of infections decreases substantially. Allowing a large number of infections can only be counterbalanced

366   by very high vaccination rates, which ensure that herd immunity is reached before the MT strain can appear and

367   takeover. Furthermore, our result underlines the importance of a worldwide effort to quickly vaccinate as many

368   individuals as possible, especially in highly populated countries with low access to vaccines. Slow, or no

369   vaccination, results in a large number of total cases in these areas and hence the emergence of an MT strain

370   which could then spread over the whole world.

371   METHODS

372

373   Derivation of mathematical results

374

375   All of the stochastic simulations presented in **Figure 3** and **Figure 4** were run with the full model presented in

376   **Figure 2**. However, in the following derivations, we make certain approximations in order to obtain analytical

377   results. Among others, we neglect death and in some cases and we neglect vaccination of recovered individuals.

378

379   1. No Vaccination

380

381   First we consider the case without vaccination. We denote by x the number of susceptible individuals; by y the

382   number of individuals infected with wildtype (WT); by z the number of individuals recovered from WT. The

383   infection rate is β; the recovery rate a ; the mutation rate μ; the population size N. The social activity parameter

384 $s(t)$ captures the extent of imposed lockdown that varies over time. For simplicity, we neglect the number of

385 individuals who die, hence the population size N is assumed to be constant.

386 Deterministic WT infection dynamics are given by the system of differential equations:

$$\dot{x} = -\beta s x y$$

$$\dot{y} = \beta s x y - a y \qquad (7)$$

$$\dot{z} = a y$$

387 Initially, all of the population is susceptible to the WT strain, and no individuals are infected with or recovered

388 from the WT strain. Therefore, we have: $x(0) = N$, $y(0) = 0$ and $z(0) = 0$. Social activity, $s(t)$, is adjusted

389 such that $y(t) = L/a$ is constant (see **Figure S2C**). L is the number of new infections per day.

390 Without lockdown, $s = 1$, the basic reproductive ratio of the WT is given by $R_0 = \beta N/a$. If $R_0 > 1$, the number

391 of infected individuals grows initially. With lockdown, $s < 1$, the reproductive ratio is $R_{WT} = \beta N s/a$. Since the

392 social distancing measures maintain $y(t) = L/a$ at a constant value, we have $R_{WT} = 1$ and $\beta s(t) x(t) = a$ (see

393 **Figure S2**). The parameter s can vary between 0 and 1.

394 Note that although R_{WT} and R_{MT} are initially equal, they are not equal at any later time point of the simulation.

395 This is because the reproductive coefficient of the WT strain and MT strain are dependent on the number of

396 individuals that can be infected by WT and the number of individuals that can be infected by MT. Initially, both

397 strains can infect the whole population. As the simulation progresses, the WT strain can infect less individuals

398 due to recovery of WT infected individuals and due to vaccination. On the other hand, the MT strain can still

399 potentially infect every individual in the population since WT-recovered individuals and vaccinated individuals

400 are susceptible to MT.

401 Each day, L individuals become infected and L individuals recover. Therefore, because of dynamic lockdown,

402 the following equation is equivalent to (7):

$$\dot{x} = -L$$

$$\dot{y} = 0 \qquad (8)$$

$$\dot{z} = L$$

403 The solution to this system of differential equations is

$$x(t) = N - Lt \qquad (9)$$

$$z(t) = Lt$$

404　Hence, the number of susceptible individuals decreases linearly with slope L while the number of recovered

405　individuals increases linearly with slope L. (See **Figure S2** for agreement with the stochastic simulation).

406　When $x(t)$ has declined such that $R_{WT} < 1$ and $s = 1$, there are not enough susceptible individuals to sustain

407　the infection. This herd immunity is achieved when $x(t) < a/\beta$. Thus, the time T_H until herd immunity is given

408　by $\beta(N - Lt) = a$. We obtain:

$$T_H = \frac{N}{L}\left(1 - \frac{1}{R_0}\right) \tag{10}$$

409　*1.1 Rate of generating mutants in absence of vaccination*

410

411　Each day, L new individuals become infected. Each of these infections has probability μ to be a vaccine-resistant

412　MT. Hence, the rate of producing a mutant is $L\mu$ per day. Let $P(t)$ denote the probability that no mutant has

413　been produced until time t. We have $\dot{P}(t) = -L\mu P(t)$, which leads to $P(t) = e^{-L\mu t}$.

414　The MT strain can be generated only during infection. Hence, if the MT strain has not been generated until the

415　time when there are no more WT infections – that is, approximately when herd immunity is reached – it will

416　never be generated. We neglect here the time of exponential decrease in the number of WT infections between

417　time T_H (when herd immunity is reached) and the time when the number of WT infections has reached zero.

418　The probability that no mutant will appear before time T_H is $P(T_H) = e^{-L\mu T_H}$. Inserting from eq (4) we obtain

$$P(T_H) = \exp\left(-N\mu\left(1 - \frac{1}{R_0}\right)\right) \tag{11}$$

419

420　*1.2 Rate of generating surviving mutants in absence of vaccination*

421

422　In order to calculate the probability that the MT strain will be generated and survive, we need to multiply the

423　rate of generation of the MT strain with the probability that it will not become extinct by random drift. If $\rho(t)$

424　is the survival probability of the MT, then the rate of producing a surviving mutant is $L\mu\rho(t)$ per day. We

425　approximate $\rho(t) = 1 - 1/R_{MT}(t)$, where $R_{MT}(t)$ is the reproductive ratio of the mutant at time T.

426　We have

$$R_{MT}(t) = \beta s(t)N/a \tag{12}$$

427 Since $s(t) = a/\beta x(t)$ and using Eq. (9) we obtain

$$R_{MT}(t) = \frac{N}{N - Lt} \tag{13}$$

428 And therefore we have $\rho(t) = Lt/N$.

429 Let $P(t)$ denote the probability that not surviving mutant has been produced until time t. We have $\dot{P}(t) =$

430 $-L\mu\rho(t)P(t) = -L^2\mu t P(t)/N$. We can solve this differential equation to obtain $P(t) = \exp(-\mu L^2 t^2/2N)$.

431 The probability that no surviving mutant has been produced until herd immunity, which is reached at time T_H,

432 is given by

$$P(T_H) = \exp(-\frac{\mu N}{2}\left(1 - \frac{1}{R_0}\right)^2) \tag{14}$$

433

434 2. With Vaccination

435

436 Let us now add vaccination. Denote by w the number of vaccinated people. If both recovered and susceptible

437 individuals are vaccinated at a total rate of c per day then deterministic infection and vaccination dynamics

438 are given by

$$\dot{x} = -\beta sxy - \frac{cx}{x + z}$$

$$\dot{y} = \beta sxy - ay$$

$$\dot{z} = ay - \frac{cz}{x + z} \tag{15}$$

$$\dot{w} = c$$

439 The initial condition is $x(0) = N$, $y(0) = 0$, $z(0) = 0$, $w(0) = 0$, $s(0) = 1$ and $R_0 = \beta N/a$. As before, we

440 adjust $s(t)$ such that $y(t) = L/a$ is constant (see **Figure 3**).

441 Each day, L susceptible individuals become infected and $cx(x + z)$ susceptible individuals become vaccinated.

442 Also, L infected individuals recover, and $cx(x + z)$ of recovered individuals become vaccinated. We have:

$$\dot{x} = -L - \frac{cx}{x + z} \tag{16}$$

$$\dot{y} = 0$$

$$\dot{z} = L - \frac{cz}{x + z}$$

$$\dot{w} = c$$

443 For simplicity let us assume that we only vaccinate susceptible people. This assumption is a reasonable
444 approximation if $c \gg L$. In this case, we can write

$$\dot{x} = -L - c$$

$$\dot{y} = 0$$

$$\dot{z} = L \tag{17}$$

$$\dot{w} = c$$

445

446 The solution to this system of differential equations is

$$x(t) = N - Lt - ct$$

$$z(t) = Lt \tag{18}$$

$$w(t) = ct$$

447 Hence, the number of susceptible individuals decreases linearly with slope $L + c$, while the number of recovered
448 individuals increases linearly with slope L, and the number of vaccinated individuals increases linearly with slope
449 c.

450 The time T_H until herd immunity is given by

$$T_H = \frac{N}{c + L}(1 - 1/R_0) \tag{19}$$

451

452 2.1 Rate of generating mutants during vaccination

453

454 The rate of producing a mutant is $L\mu$ per day. Let $P(t)$ denote the probability that no mutant has been produced
455 until time t. We have $\dot{P}(t) = -L\mu P(t)$, which gives $P(t) = \exp(-L\mu t)$.

456 The MT strain can be generated only during infection. Hence, if the MT strain has not been generated until the

457 time when there are no more WT infections – that is, when herd immunity is reached – it will never be

458 generated. Again we neglect here the time of exponential decrease in the number of WT infections between

459 the time T_H when herd immunity is reached and the time where the number of WT infections reaches 0. Hence,

460 the probability that no mutant will appear is $P(T_H) = \exp(-L\mu T_H)$. Using Eq. (19), the probability that no

461 mutant has appeared until herd immunity is:

$$P(T_H) = \exp(-N\mu \left(\frac{L}{c+L}\right)\left(1 - \frac{1}{R_0}\right))$$

(20)

462 ## 2.2 Rate of generating surviving mutants during vaccination

463

464 In order to calculate the probability that surviving mutants are generated, we again consider the survival

465 probability $\rho(t) = 1 - 1/R_{MT}(t)$, where $R_{MT}(t)$ is the reproductive ratio of the mutant at time t. The rate of

466 producing a surviving mutant is then $L\mu\rho(t)$ per day. We have:

$$R_{MT}(t) = \frac{\beta s(t)N}{a}$$

(21)

467 As explained above, $s(t) = a/\beta x(t)$. Using Eq. (18) we obtain

$$R_{MT}(t) = \frac{N}{N - (L+c)t}$$

(22)

468 And therefore $\rho(t) = (L+c)t/N$.

469 Let $P(t)$ denote the probability that not surviving mutant has been produced until time t. We have $\dot{P}(t) =$

470 $-L\mu\rho(t)P(t) = -L\mu(c+L)tP(t)/N$. Let $v = c/N$ and $l = L/N$. We can solve this differential equation to

471 obtain:

$$P(t) = \exp(-\frac{\mu N}{2}l(v+l)t^2)$$

(23)

472 The probability that no surviving mutant has been produced until herd immunity, which is reached at time T_H,

473 is:

$$P(T_H) = \exp(-\frac{\mu N}{2}(\frac{l}{v+l})\left(1 - \frac{1}{R_0}\right)^2)$$

(24)

474

475

476   ## 2.3 Rate of generating surviving mutants with partial immune escape during vaccination

477

478   We can also study the case where the infectivity of the mutants is reduced by a factor $q \in [0,1]$ when infecting

479   recovered or vaccinated people. For $q = 1$ we obtain full escape, while $q = 0$ means that the mutant does not

480   escape at all.

481   A similar derivation to the one above leads to the following result. The probability that no surviving mutant

482   with partial escape q has appeared until herd immunity is given by:

$$P(T_H) = \exp(-\frac{\mu N}{2} (\frac{l}{v+l})A)$$

with $\qquad A = \frac{2q}{1-q}(-\frac{R_0-1}{R_0} + \frac{1}{1-q}\log\frac{R_0}{1+q(R_0-1)})$ $\qquad$ (25)

483   For $q = 1$ we obtain $A = (1 - (1/R_0))^2$ leading to Eq. (23) above.

484

485

486

487

488

489   Relationship between the product formula and the exponential formula

490

491   Each day, L new WT infections occur. Each new infection has a probability of μ to be the MT strain. The survival

492   probability of the mutant is approximately $1 - 1/R_m(t)$ where $R_m(t)$ is the basic reproductive ratio of the MT

493   appearing at time t.

494   Hence, the probability that none of the L new WT infections in a day will generate a surviving mutant is

495    $(1 - \mu(1 - 1/R_m(t)))^L$. Then, we can write the probability P that no surviving mutant will be produced

496   between time $t = 0$ and the time T_H when herd immunity is reached as the product

$$P = \prod_{\tau=0}^{T_H}[1 - \mu\left(1 - \frac{1}{R_{MT}(\tau)}\right)]^L$$ $\qquad$ (26)

497   We have $T_H = [N/(c + L)](1 - 1/R_0)$ and $R_{MT}(t) = N/[N - (c + L)t]$.

498   Since $\rho(t) = 1 - 1/R_m(t) = (c + L)t/N$ we can write:

499
$$P = \prod_{\tau=0}^{T_H} (1 - \frac{\mu(c + L)\tau}{N})^L$$

500   Let us use the abbreviation $u = \mu(c + L)/N$. Then

501
$$P = \prod_{\tau=0}^{T_H} (1 - u\tau)^L$$

502
$$= \exp[log \prod_{\tau=0}^{T_H} (1 - u\tau)^L]$$

503
$$= \exp[L\ log \prod_{\tau=0}^{T_H} (1 - u\tau)]$$

$$= \exp[L \sum_{\tau=0}^{T_H} log(1 - u\tau)] \tag{27}$$

504   Note that Eq. (26) is exactly equivalent to Eq. (23). Assuming $uT_H \ll 1$ which is the same as $\mu(1 - (1/R_0)) \ll 1$
505   we obtain

506
$$P = \exp[-uL \sum_{\tau=0}^{T_H} \tau]$$

507
$$= \exp\left[-\frac{uLT_H(T_H + 1)}{2}\right]$$

508   Assuming $T_H \gg 1$ which is $N\left(1 - \frac{1}{R_0}\right) \gg c + L$, we obtain

509
$$P = \exp\left[-\frac{uLT_H^2}{2}\right]$$

510
$$= \exp\left[-\frac{(\mu(c + L)/N)LT_H^2}{2}\right]$$

511   Finally, inserting $T_H = (N/(c + L))(1 - 1/R_0)$ we get:

$$P(T_H) = \exp(-\frac{\mu N}{2}(\frac{l}{v + l})\left(1 - \frac{1}{R_0}\right)^2) \tag{28}$$

512   Which is equivalent to Eq.(24) (see above).

513

514   Dynamics after appearance of the MT strain

515

516   1. No Vaccination

517

518   After the MT strain has taken over, social distancing measures will continue maintaining the number of daily

519   infections at L, which implies that $(y_1 + y_2) = L/a$ (see **Figure S2**). In practice, the WT strain rapidly goes extinct

520   upon emergence of the MT strain; so we can consider $y_2 = L/a$. The mutant strain can infect susceptible

521   individuals x, and recovered individuals, z_1. The mutant strain infects those individuals with probabilities

522   proportional to their frequencies at the time t^* of mutant takeover. Hence, for times $t > t^*$ we have:

$$x(t) = x(t^*) - \frac{x(t^*)}{z_1(t^*) + x(t^*)} L(t^* - t)$$

(29)

$$z_1(t) = z_1(t^*) - \frac{z_1(t^*)}{z_1(t^*) + x(t^*)} L(t^* - t)$$

523   After mutant takeover, the social distancing measures need to be readjusted to the mutant strain. Since more

524   individuals are susceptible to it, $s(t)$ has to decrease (see **Figure S2F**):

$$s(t) = \frac{aN}{\beta(x(t) + qz_1(t))}$$

(30)

525   Which implies that $R_{MT} = 1$.

526

527   2. With vaccination

528

529   As for the case without vaccination, if the mutant strain survives, it will quickly replace the wild-type strain such

530   that $y_2 = L/a$ (see **Figure 3C**). The number of susceptible individuals $x(t^*)$ at time of mutant takeover can be

531   neglected for large enough vaccination rates. The number of vaccinated individuals, susceptible to the mutant

532   strain w_1 will hence decrease linearly with the number of tolerated cases per day L, and the number of

533   vaccinated individuals, recovered from the mutant strain w_2 will increase complementarily linearly with L. If the

534   mutant takes over at time t^*, we have for all times $t > t^*$:

$$w_1(t) = w_1(t^*) - L(t^* - t)$$
(31)

$$w_2(t) = L(t^* - t)$$

535   The social activity parameter s needs readjustment to consider the additional groups of individuals that are now

536   susceptible to the infecting strain. We have:

$$s(t) = \frac{a}{\beta} \frac{x(t) + q(z_1(t) + w_1(t))}{x(t) + q(z_1(t) + w_1(t)) - w_2(t)} \tag{32}$$

537   Which ensures that $R_{MT} = 1$. Here the parameter q in $[0,1]$ denotes the extent of escape.

538

539   Estimating the evolutionary potential of the virus

540

541   If μ is the mutation rate as described above and $L(t)$ is the time series giving the number of new infections on

542   day t, then the probability that no mutant has been produced between time 0 and time T_H is given by:

$$P(T_H) = \prod_{\tau=0}^{T_H} [1 - \mu]^{L(\tau)} \tag{33}$$

543   This probability will overestimate the evolutionary potential of the virus to escape from vaccination because

544   many mutants do not survive the initial random drift. The probability that no surviving mutant has been

545   produced between time 0 and time T_H can be written as:

$$P(T_H) = \prod_{\tau=0}^{T_H} [1 - \mu\rho(\tau)]^{L(\tau)} \tag{34}$$

546   Here $\rho(t)$ is the survival probability of an escape mutant produced at time t. This probability depends on the

547   basic reproductive ratio of the mutant on the day it is being produced (and the next few days until random drift

548   is negligible). Approximately we can write:

$$\rho(t) = \min\{0,1 - \frac{1}{R_M(t)}\} \tag{35}$$

549   For the potential of the virus to generate mutants (irrespective of whether they survive) what matters most is

550   the total number of infections, $\sum_\tau L(\tau)$. But for the potential of the virus to generate surviving mutants one

551   must also consider the time periods when lockdown is relaxed such that R_{MT} is above 1.

552

553

Analytic approximation for more infectious, vaccine escape mutants

554

555

1. No Vaccination

556

557

558 Now we calculate the probability that mutants are being generated which do become extinct by random drift.

559 We denote f the relative infectiousness of the mutant vs. the wild type strain. Hence, for more infectious

560 mutants, we have $f > 1$.

561 The rate of producing a surviving mutant is $L\mu\rho(t)$ per day. Here $\rho(t)$ is the survival probability, given by

562 $\rho(t) = 1 - 1/R_M(t)$. The basic reproductive ratio of the mutant at time t is: $R_M(t) = f\beta s(t)N/a$. Since we

563 have $\beta s(t)N/a = 1/x(t)$. We have $R_M(t) = fN/(N - Lt)$ and therefore:

$$\rho(t) = 1 - \frac{1}{R_M(t)} = \frac{N(f - 1) + Lt}{Nf} \tag{36}$$

564 Let $P(t)$ denote the probability that no surviving mutant has been produced until time t.

565 We have $\dot{P}(t) = -L\mu\rho(t)P(t)$. Thus, $\dot{P}(t) = (\kappa + \lambda t)P(t)$, with the solution $P(t) = \exp(\kappa t + \frac{\lambda}{2}t^2)$.

566 Which already leads to $P(0) = 1$ as desired. In our original notation, the solution becomes:

$$P(t) = \exp(-L\mu\frac{N(f - 1)}{Nf}t - L\mu\frac{Lt}{2Nf}t^2) \tag{37}$$

567

568

569

570

2. With vaccination

571

572

573 The rate of producing a surviving mutant is $L\mu\rho(t)$ per day. Here $\rho(t)$ is the survival probability given by

574 $\rho(t) = 1 - 1/R_m(t)$. The basic reproductive ratio of the mutant at time t is $R_M(t) = f\beta s(t)N/a$. Since

575 $\beta s(t)N/a = 1/x(t)$. We have $R_M(t) = fN/[N - (c + L)t]$ and:

$$\rho(t) = 1 - \frac{1}{R_M(t)} = \frac{N(f - 1) + (c + L)t}{Nf} \tag{38}$$

Let $P(t)$ denote the probability that no surviving mutant has been produced until time t. We have $\dot{P}(t) = -L\mu\rho(t)P(t)$. Thus:

$$\dot{P}(t) = -L\mu\frac{N(f-1)+(c+L)t}{Nf}P(t) \tag{39}$$

This solution of this differential equation is given by:

$$P(t) = \exp(-L\mu\frac{f-1}{f}t - L\mu\frac{c+L}{2Nf}t^2) \tag{40}$$

REFERENCES

[1]   J. T. Wu *et al.*, "Estimating clinical severity of COVID-19 from the transmission dynamics in Wuhan, China," *Nat. Med.*, 2020, doi: 10.1038/s41591-020-0822-7.

[2]   "COVID-19 Data Explorer - Our World in Data." https://ourworldindata.org/explorers/coronavirus-data-explorer?zoomToSelection=true&time=2020-03-01..latest&country=USA~GBR~CAN~DEU~ITA~IND&region=World&pickerMetric=location&pickerSort=asc&Metric=Confirmed+cases&Interval=7-day+rolling+average&Align+outbreaks=false&Relative+to+Population=true (accessed Mar. 19, 2021).

[3]   "Different COVID-19 Vaccines | CDC." https://www.cdc.gov/coronavirus/2019-ncov/vaccines/different-vaccines.html (accessed Mar. 19, 2021).

[4]   "Safe COVID-19 vaccines for Europeans | European Commission." https://ec.europa.eu/info/live-work-travel-eu/coronavirus-response/safe-covid-19-vaccines-europeans_en (accessed Mar. 19, 2021).

[5]   L. Böttcher and J. Nagler, "Decisive Conditions for Strategic Vaccination against SARS-CoV-2," *medRxiv*, p. 2021.03.05.21252962, Mar. 2021, doi: 10.1101/2021.03.05.21252962.

[6]   E. E. Walsh, J. H. Shin, and A. R. Falsey, "Clinical impact of human coronaviruses 229E and OC43 infection in diverse adult populations," *J. Infect. Dis.*, 2013, doi: 10.1093/infdis/jit393.

[7]   "Vaccines – COVID19 Vaccine Tracker." https://covid19.trackvaccines.org/vaccines/ (accessed Mar. 19, 2021).

[8]   H. Tegally *et al.*, "Emergence and rapid spread of a new severe acute respiratory syndrome-related coronavirus 2 (SARS-CoV-2) lineage with multiple spike mutations in South Africa," *medRxiv*, vol. 10. medRxiv, p. 2020.12.21.20248640, Dec. 22, 2020, doi: 10.1101/2020.12.21.20248640.

[9]   A. Rambaut *et al.*, "Preliminary genomic characterisation of an emergent SARS-CoV-2 lineage in the UK defined by a novel set of spike mutations - SARS-CoV-2 coronavirus / nCoV-2019 Genomic Epidemiology - Virological," 2020. https://virological.org/t/preliminary-genomic-characterisation-of-an-emergent-sars-cov-2-lineage-in-the-uk-defined-by-a-novel-set-of-spike-mutations/563 (accessed Apr. 16, 2021).

[10]   P. Wang *et al.*, "Increased Resistance of SARS-CoV-2 Variants B.1.351 and B.1.1.7 to Antibody Neutralization.," *bioRxiv Prepr. Serv. Biol.*, 2021, doi: 10.1101/2021.01.25.428137.

[11]   L. L. Luchsinger and C. D. Hillyer, "Vaccine efficacy probable against COVID-19 variants," *Science (80-.).*, vol. 371, no. 6534, pp. 1116 LP – 1116, Mar. 2021, doi: 10.1126/science.abg9461.

[12]   T. N. Starr *et al.*, "Prospective mapping of viral mutations that escape antibodies used to treat COVID-19," *Science (80-.).*, vol. 371, no. 6531, pp. 850–854, Feb. 2021, doi: 10.1126/science.abf9302.

[13]   T. N. Starr *et al.*, "Deep Mutational Scanning of SARS-CoV-2 Receptor Binding Domain Reveals Constraints on

611   Folding and ACE2 Binding," *Cell*, vol. 182, no. 5, pp. 1295-1310.e20, Sep. 2020, doi: 10.1016/j.cell.2020.08.012.

612   [14]   A. J. Greaney *et al.*, "Complete Mapping of Mutations to the SARS-CoV-2 Spike Receptor-Binding Domain that
613   Escape Antibody Recognition," *Cell Host Microbe*, vol. 29, no. 1, pp. 44-57.e9, Jan. 2021, doi:
614   10.1016/j.chom.2020.11.007.

615   [15]   R. N. Thompson, E. M. Hill, and J. R. Gog, "SARS-CoV-2 incidence and vaccine escape," *Lancet Infect. Dis.*, Apr.
616   2021, doi: 10.1016/S1473-3099(21)00202-4.

617   [16]   P. J. Gerrish, F. Saldaña, B. Galeota-Sprung, A. Colato, E. E. Rodriguez, and J. X. V. Hernández, "How unequal
618   vaccine distribution promotes the evolution of vaccine escape," *medRxiv*, 2021.

619   [17]   S. Cobey, D. B. Larremore, Y. H. Grad, and M. Lipsitch, "Concerns about SARS-CoV-2 evolution should not hold
620   back efforts to expand vaccination," *Nature Reviews Immunology*. Nature Research, pp. 1–6, Apr. 01, 2021, doi:
621   10.1038/s41577-021-00544-9.

622   [18]   F. Geoffroy, A. Traulsen, and H. Uecker, "Vaccination strategies when vaccines are scarce: On conflicts between
623   reducing the burden and avoiding the evolution of escape mutants," *medRxiv*, p. 2021.05.04.21256623, May
624   2021, doi: 10.1101/2021.05.04.21256623.

625   [19]   R. E. Baker, W. Yang, G. A. Vecchi, C. J. E. Metcalf, and B. T. Grenfell, "Assessing the influence of climate on
626   wintertime SARS-CoV-2 outbreaks," *Nat. Commun.*, vol. 12, no. 1, pp. 1–7, Dec. 2021, doi: 10.1038/s41467-021-
627   20991-1.

628   [20]   J. L. Geoghegan *et al.*, "Genomic epidemiology reveals transmission patterns and dynamics of SARS-CoV-2 in
629   Aotearoa New Zealand," *Nat. Commun.*, vol. 11, no. 1, pp. 1–7, Dec. 2020, doi: 10.1038/s41467-020-20235-8.

630   [21]   A. B. Komissarov *et al.*, "Genomic epidemiology of the early stages of the SARS-CoV-2 outbreak in Russia," *Nat.
631   Commun.*, vol. 12, no. 1, pp. 1–13, Dec. 2021, doi: 10.1038/s41467-020-20880-z.

632   [22]   N. R. Faria *et al.*, "Genomics and epidemiology of the P.1 SARS-CoV-2 lineage in Manaus, Brazil," *Science (80-.).*,
633   p. eabh2644, Apr. 2021, doi: 10.1126/science.abh2644.

634   [23]   K. A. Lythgoe *et al.*, "SARS-CoV-2 within-host diversity and transmission," *Science (80-.).*, vol. 372, no. 6539, p.
635   eabg0821, Mar. 2021, doi: 10.1126/science.abg0821.

636   [24]   N. L. Komarova, L. M. Schang, and D. Wodarz, "Patterns of the COVID-19 pandemic spread around the world:
637   Exponential versus power laws: Patterns of the COVID-19 pandemic spread around the world: Exponential versus
638   power laws," *J. R. Soc. Interface*, vol. 17, no. 170, Sep. 2020, doi: 10.1098/rsif.2020.0518.

639   [25]   C. M. Saad-Roy *et al.*, "Immune life history, vaccination, and the dynamics of SARS-CoV-2 over the next 5 years,"
640   *Science (80-.).*, vol. 370, no. 6518, pp. 811–818, Nov. 2020, doi: 10.1126/science.abd7343.

641   [26]   BERNOULLI and D., "Essai d'une nouvelle analyse de la mortalite causee par la petite verole, et des avantages de
642   l'inoculation pour la prevenir," *Hist. l'Acad., Roy. Sci. avec Mem*, pp. 1–45, 1760, Accessed: Mar. 30, 2021.
643   [Online]. Available: https://ci.nii.ac.jp/naid/10013124549.

644   [27]   W. 0 Kermack and A. G. Mckendrick, "A contribution to the mathematical theory of epidemics," *Proc. R. Soc.
645   London. Ser. A, Contain. Pap. a Math. Phys. Character*, vol. 115, no. 772, pp. 700–721, Aug. 1927, doi:
646   10.1098/rspa.1927.0118.

647   [28]   O. Diekmann, J. A. P. Heesterbeek, and J. A. J. Metz, "On the definition and the computation of the basic
648   reproduction ratio R0 in models for infectious diseases in heterogeneous populations," *J. Math. Biol.*, vol. 28, no.
649   4, pp. 365–382, 1990, doi: 10.1007/BF00178324.

650   [29]   K. Dietz, "The estimation of the basic reproduction number for infectious diseases," *Stat. Methods Med. Res.*, vol.
651   2, no. 1, pp. 23–41, Mar. 1993, doi: 10.1177/096228029300200103.

652   [30]   M. A. Nowak and R. M. May, "Superinfection and the evolution of parasite virulence," *Proc. R. Soc. B Biol. Sci.*,
653   vol. 255, no. 1342, pp. 81–89, 1994, doi: 10.1098/rspb.1994.0012.

[31] M. A. Nowak and C. R. M. Bangham, "Population dynamics of immune responses to persistent viruses," *Science (80-.).*, vol. 272, no. 5258, pp. 74–79, 1996, doi: 10.1126/science.272.5258.74.

[32] H. W. Hethcote, "Mathematics of infectious diseases," *SIAM Rev.*, vol. 42, no. 4, pp. 599–653, 2000, doi: 10.1137/S0036144500371907.

[33] F. Brauer and C. Castillo-Chavez, *Mathematical Models in Population Biology and Epidemiology*, vol. 40. New York, NY: Springer New York, 2012.

[34] W. Hamer, "The Milroy Lectures ON EPIDEMIC DISEASE IN ENGLAND-THE EVIDENCE OF VARIABILITY AND OF PERSISTENCY OF TYPE.," *The Lancet*, vol. 167, no. 4305. Elsevier, pp. 569–574, Mar. 03, 1906, doi: 10.1016/S0140-6736(01)80187-2.

[35] N. Bailey, "The Mathematical Theory of Infectious Diseases and its applications," Wiley-Blackwell, 1978. Accessed: Mar. 30, 2021. [Online]. Available: https://www.ncbi.nlm.nih.gov/pmc/articles/PMC1457188/.

[36] H. E. Tillett, "Infectious Diseases of Humans; Dynamics and Control," *Epidemiol. Infect.*, vol. 108, no. 1, p. 211, 1992, Accessed: Mar. 30, 2021. [Online]. Available: https://www.ncbi.nlm.nih.gov/pmc/articles/PMC2272191/.

[37] M. Nowak and R. M. May, "Virus Dynamics: Mathematical Principles of Immunology And Virology." https://www.researchgate.net/publication/48378467_Virus_Dynamics_Mathematical_Principles_of_Immunology_And_Virology (accessed Mar. 30, 2021).

[38] O. Diekmann and J. A. P. Heesterbeek, "Mathematical Epidemiology of Infectious Diseases: Model Building, Analysis and Interpretation." https://www.researchgate.net/publication/48376881_Mathematical_Epidemiology_of_Infectious_Diseases_Model_Building_Analysis_and_Interpretation (accessed Mar. 30, 2021).

[39] M. Ragonnet-Cronin *et al.*, "Genetic evidence for the association between COVID-19 epidemic severity and timing of non-pharmaceutical interventions," *Nat. Commun.*, vol. 12, no. 1, p. 2188, Dec. 2021, doi: 10.1038/s41467-021-22366-y.

[40] H. Rossman *et al.*, "Hospital load and increased COVID-19 related mortality in Israel," *Nat. Commun.*, vol. 12, no. 1, p. 1904, Dec. 2021, doi: 10.1038/s41467-021-22214-z.

[41] C. M. Saad-Roy *et al.*, "Epidemiological and evolutionary considerations of SARS-CoV-2 vaccine dosing regimes," *Science (80-.).*, p. eabg8663, Mar. 2021, doi: 10.1126/science.abg8663.

[42] C. M. Saad-Roy *et al.*, "Immune life history, vaccination, and the dynamics of SARS-CoV-2 over the next 5 years," *Science (80-.).*, vol. 370, no. 6518, pp. 811–818, Nov. 2020, doi: 10.1126/science.abd7343.

[43] P. Ashcroft, S. Lehtinen, D. C. Angst, N. Low, and S. Bonhoeffer, "Quantifying the impact of quarantine duration on covid-19 transmission," *Elife*, vol. 10, pp. 1–33, Feb. 2021, doi: 10.7554/eLife.63704.

[44] N. L. Komarova, A. Azizi, and D. Wodarz, "Network models and the interpretation of prolonged infection plateaus in the COVID19 pandemic," *Epidemics*, p. 100463, May 2021, doi: 10.1016/j.epidem.2021.100463.

[45] M. Castro, S. Ares, J. A. Cuesta, and S. Manrubia, "The turning point and end of an expanding epidemic cannot be precisely forecast," *Proc. Natl. Acad. Sci.*, vol. 117, no. 42, pp. 26190–26196, Oct. 2020, doi: 10.1073/PNAS.2007868117.

[46] M. Stich, S. C. Manrubia, and E. Lázaro, "Variable mutation rates as an adaptive strategy in replicator populations," *PLoS One*, 2010, doi: 10.1371/journal.pone.0011186.

[47] O. Yagan, A. Sridhar, R. Eletreby, S. A. Levin, J. B. Plotkin, and H. V. Poor, "Modeling and Analysis of the Spread of COVID-19 Under a Multiple-Strain Model with Mutations," *Harvard Data Sci. Rev.*, 2021, doi: 10.1162/99608f92.a11bf693.

[48] S. Lehtinen, P. Ashcroft, and S. Bonhoeffer, "On the relationship between serial interval, infectiousness profile and generation time," *J. R. Soc. Interface*, 2021, doi: 10.1098/rsif.2020.0756.

697   [49]   H. W. Hethcote, "Three Basic Epidemiological Models," 1989.

698   [50]   D. T. Gillespie, "A general method for numerically simulating the stochastic time evolution of coupled chemical
699   reactions," *J. Comput. Phys.*, vol. 22, no. 4, pp. 403–434, Dec. 1976, doi: 10.1016/0021-9991(76)90041-3.

700   [51]   D. T. Gillespie, "Exact stochastic simulation of coupled chemical reactions," in *Journal of Physical Chemistry*, 1977,
701   vol. 81, no. 25, pp. 2340–2361, doi: 10.1021/j100540a008.

702   [52]   W. Cota and S. C. Ferreira, "Optimized Gillespie algorithms for the simulation of Markovian epidemic processes
703   on large and heterogeneous networks," *Comput. Phys. Commun.*, vol. 219, pp. 303–312, Oct. 2017, doi:
704   10.1016/j.cpc.2017.06.007.

705   [53]   R. I. Mukhamadiarov *et al.*, "Social distancing and epidemic resurgence in agent-based susceptible-infectious-
706   recovered models," *Sci. Rep.*, vol. 11, no. 1, p. 130, Dec. 2021, doi: 10.1038/s41598-020-80162-y.

707

708

709

710

711

712

713

714

715

716

717

718

719

720

721

722

723

724

725

726

727

728

729

730   TABLES

731

Parameter	Symbol	Biologically Significant Range	References/Notes
Wildtype R_0	β_1	$[1.8 - 3.6]$	[50]
Mutant R_0	β_2	$[1.8 - 3.6]$ $[3.6\text{-}7.2]$ (more infectious variants)	[50], [51]
Recovery Rate	a	$[0.38 - 0.08]$	[52]
Social Distancing Parameter	s	$[0.05, 1]$	-
Death Rate	d	$[0.005 - 0.02]$	[2]
Population Size	N	$> 10^6$	-
Partial Immunity Coefficient	q	$[0,1]$	-
Mutation Rate	μ	$< 10^{-6}$	This mutation rate is the composite mutation rate from a vaccine sensitive phenotype to a vaccine resistant phenotype. See section: "Estimating the mutation rate μ for estimate.
Number of Vaccinated per day per million	c	$[0 - 10,000]$	[2]
Number of Infected per day per million	L	$10 - 1000$	[2]

732

733   **Table 1: Summary of model's parameters and their biologically significant ranges.** The mutation rate refers to the
734   probability that someone infected with the wild type strain gives rise to someone infected with a vaccine resistant
735   strain. Hence, its value is different from the SARS-COV2 molecular mutation rate that occurs during one replication
736   cycle.

737

738

739

740

741

742

743

744

745

746

Rate of infection l per day per person ($\times 10^{-6}$)	Rate of vaccination c per day per person ($\times 10^{-6}$)	Time to herd immunity, T_H (in days)	Probability of resistance			
			t = 50 days	t = 100 days	t = 200 days	t = T_H
100	1000	606	0.001	0.005	0.022	0.183
100	5000	131	0.006	0.025	-	0.043
100	10,000	66	0.013	-	-	0.022
200	1000	556	0.003	0.012	0.047	0.310
200	5000	128	0.013	0.051	-	0.082
200	10,000	65	0.025	-	-	0.043
500	1000	444	0.009	0.037	0.139	0.532
500	5000	121	0.034	0.128	-	0.183
500	10,000	63	0.064	-	-	0.100

$$N = 10^8; \mu = 10^{-7}$$

Rate of infection l per day per person ($\times 10^{-6}$)	Rate of vaccination c per day per person ($\times 10^{-6}$)	Time to herd immunity, T_H (in days)	Probability of resistance			
			t = 50 days	t = 100 days	t = 200 days	t = T_H
100	1000	606	0.014	0.054	0.197	0.867
100	5000	131	0.062	0.225	-	0.353
100	10,000	66	0.119	-	-	0.197
200	1000	556	0.030	0.113	0.381	0.975
200	5000	128	0.122	0.405	-	0.575
200	10,000	65	0.225	-	-	0.353
500	1000	444	0.089	0.313	0.777	0.999
500	5000	121	0.291	0.747	-	0.867
500	10,000	63	0.481	-	-	0.652

$$N = 10^9; \mu = 10^{-7}$$

747

748 **Table 2: Calculated probability of vaccine resistance for a range of vaccination rates and infection rates.** We observe of
749 counterintuitive effect of higher probability of resistance along time for higher vaccination rates, but lower probability of
750 resistance overall. See also Figure S4.

751

752

Country	Population size $(\times 10^6)$	Average rate of infection per day per person before vaccination $(\times 10^{-6})$	Average rate of infection per day per person after vaccination $(\times 10^{-6})$	Average rate of vaccination per day per person $(\times 10^{-6})$	Probability of resistance $(\mu = 10^{-7})$
Brazil	212.6	128	259	3546	0.208
France	68.1	141	267	5142	0.125
Germany	83.8	64	117	5067	0.043
Israel	8.7	160	273	5853	0.026
United Kingdom	67.9	109	265	5819	0.157
United States	331.0	200	240	4907	0.454

753

754 **Table 3: Calculated probability of emergence of vaccine resistance using real-world data from six countries: Brazil,**
755 **France, Germany, Israel, the United Kingdom and the United States.** The probability of vaccine resistance was
756 calculated using the product formula in Eq. 2 and the data presented in Figure 5 assuming $\mu = 10^{-7}$.

757
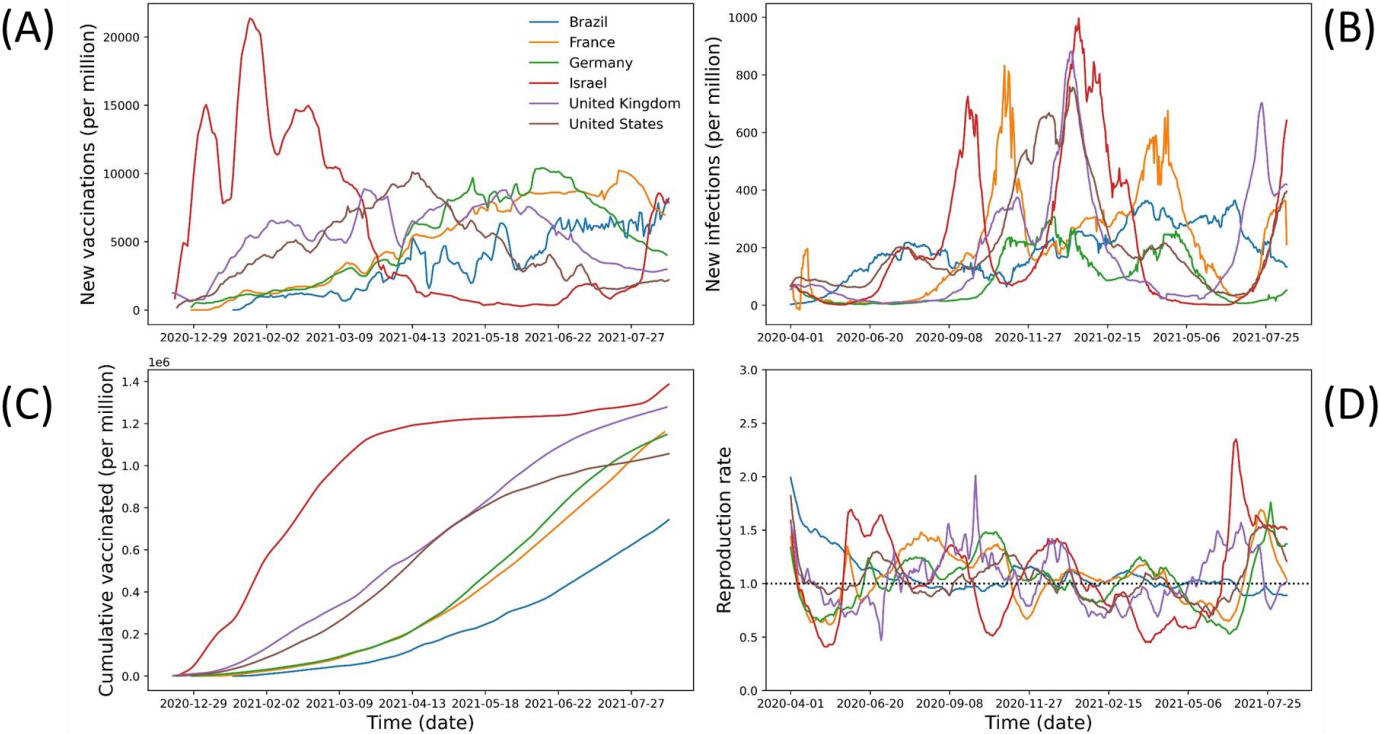
758

759

760

761

762

763

764

765

766

767

768

770

771

Figure 1: Vaccination, infection and basic reproductive ratio of SARS-CoV2 for Brazil, France, Germany, Israel, UK and USA. (A) Large scale vaccination programs commenced in December 2020. At the peak, Israel vaccinated more than 20,000 people per million (2%) per day. The vaccination rate decreased in April 2021 after most eligible individuals had been vaccinated. **(B)** In an attempt to balance economic and sanitary considerations, these six countries have gone through several cycles of loosening and tightening government-imposed restrictions, resulting in periodical increases and decreases in the number of new infections per day. The so-called "British variant", identified in November 2020, is most probably responsible for the increase in the number of infections in the UK and Israel at that time. The fourth wave in Israel (starting in July 2021) has been attributed to a combination of the emergence of the "Delta variant" and waning of immunity after vaccination. **(C)** Vaccination in most countries follows a logistic-shaped curve. At first, priority groups are vaccinated. Then, most of the population is vaccinated in a short timeframe (exponential growth). Lastly, the total number of vaccinated individuals plateaus due to vaccine hesitancy/ineligibility of the remaining non-vaccinated individuals. **(D)** The reproductive rate of SARS-COV2 infectious has hovered around 1 in the six considered countries due to the imposition of NPIs to curb the infection rates. Hence, the number of infections per day has fluctuated around an average for the duration of the pandemic.
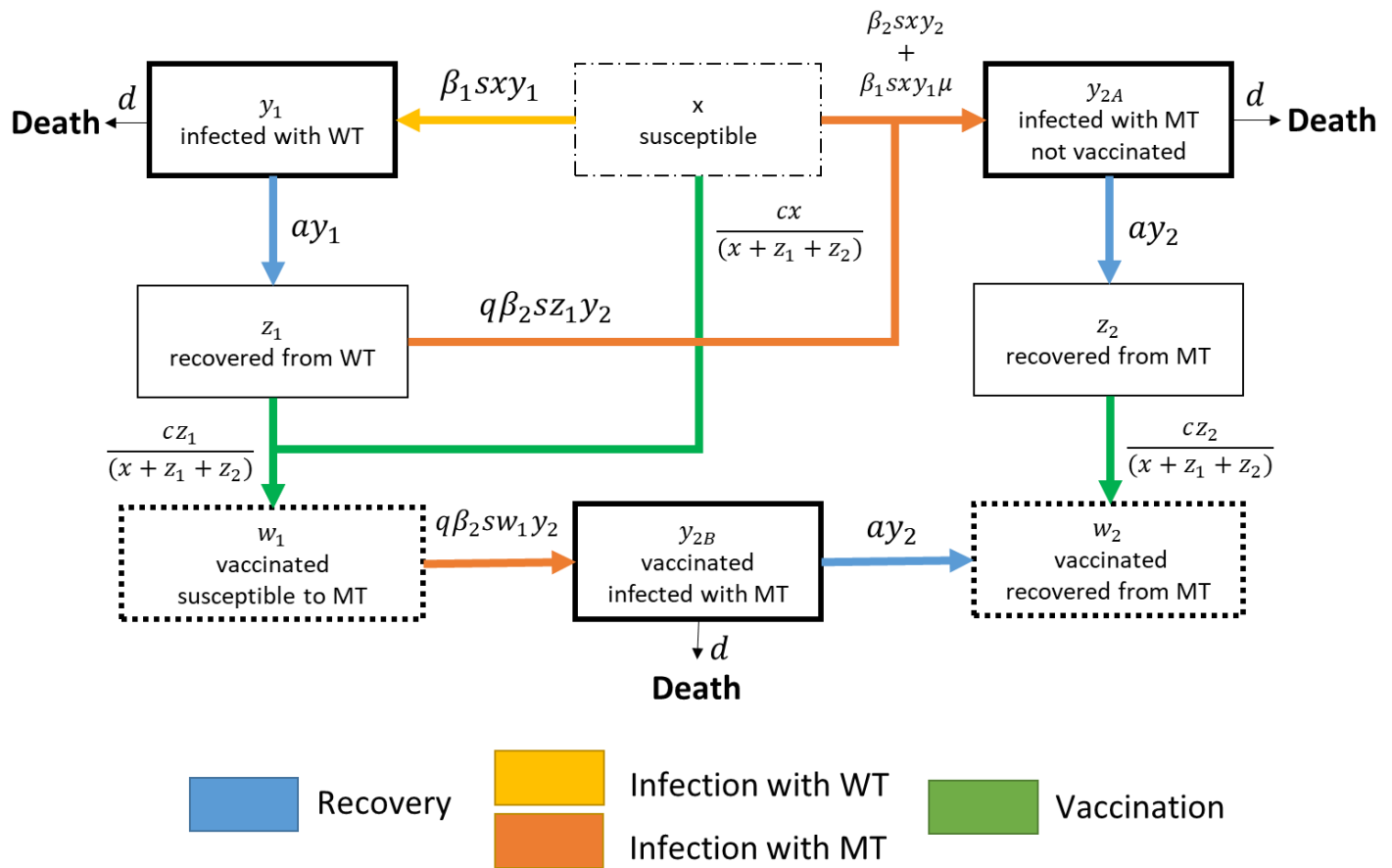
787

788

789

790

791

Figure 2: Infection dynamics, vaccination and resistance. Susceptible individuals (x) can be infected by wildtype (WT) or mutant (MT) virus. Infected people (y_1, y_{2A}, y_{2B}) die (at rate d) or recover (at rate a). People recovered from WT or vaccinated against WT can be infected by MT. People recovered from MT cannot be infected by WT. In our simplest model, we assume equal infectivity, recovery and death rates for both WT and MT. Vaccination occurs at rate c per day for all unvaccinated individuals (excluding those that are currently in active infection). Mutation happens (at rate μ) when exposure to a WT infected individual (y_1) results in the generation of a MT infected individual. Note that when exposure to a WT infected individual (y_1) results in the generation of a WT infected individual, the rate of infection should be multiplied by $1 - \mu$ in order to conserve the sum of mutation probabilities at 1. However, since μ is small, we neglect the term $1 - \mu$. The rates of these events are indicated on the arrows and are used in the Gillespie algorithm implementing stochastic dynamics.
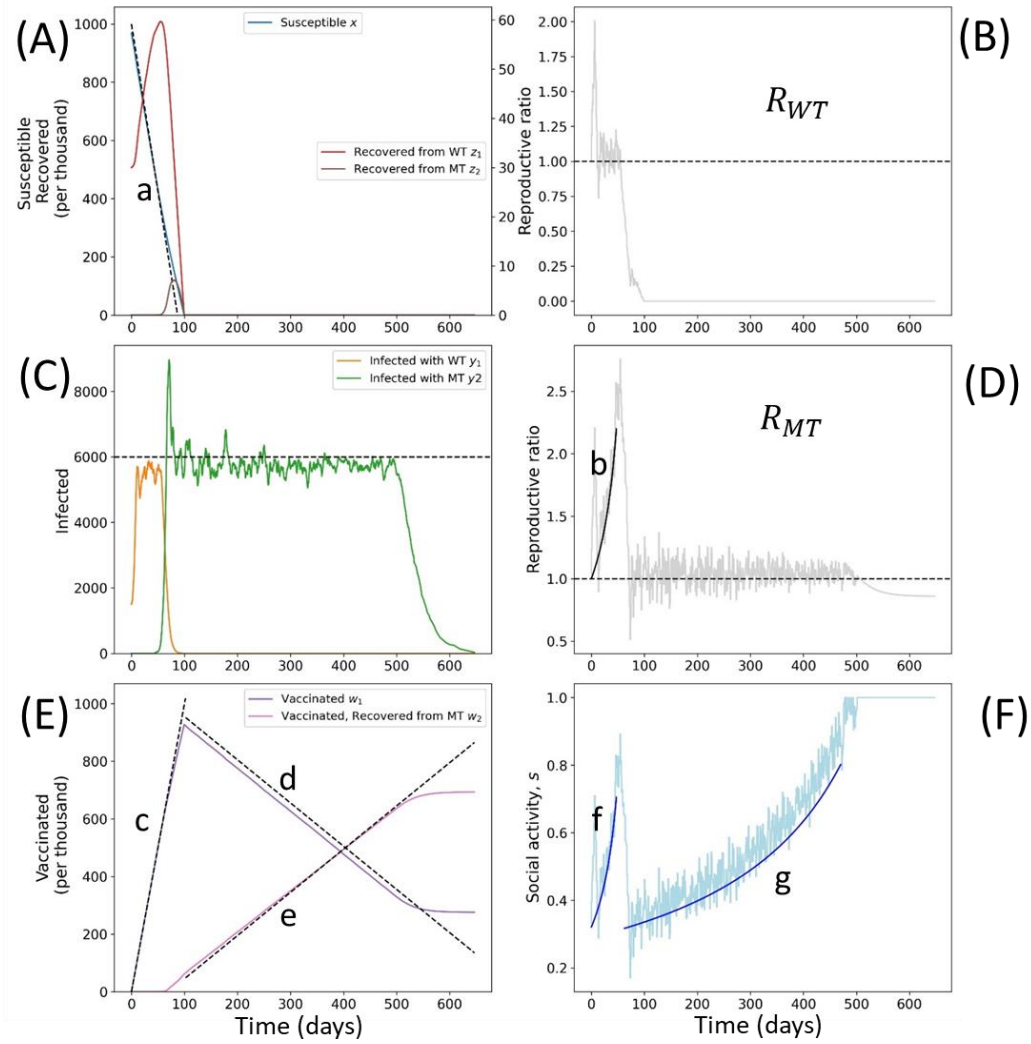
810

Figure 3: Evolution of resistance in presence of vaccination. (A) Before MT takeover, the decline in susceptible individuals (x) can be approximated by a linear function with slope equal to the vaccination rate c. Since vaccination is fast, individuals recovered from WT and non-vaccinated individuals recovered from MT are few. The equation of line (a) is $x(t) = x(0) - ct$ for $t < t^*$ where t^* is the time of takeover of the MT. (B) The reproductive rate R_{WT} is maintained at around 1 by dynamic lockdown. After mutant takeover, R_{WT} is less than 1, since the lockdown is now adjusted to the population susceptible to the MT strain. (C) The number of active WT infections before takeover and of active MT infections after takeover, is fluctuating around L/a until herd immunity to the MT is reached. (D) Before MT takeover, the reproductive rate of the MT grows as (b) $R_{MT} = \beta_2(x(t) + z_1(t) + w_1(t))/a$. After takeover, R_{MT} is maintained around 1. (E) The number of vaccinated individuals (w_1) first increases linearly with slope equal to the vaccination rate. After MT takeover, the number of individuals vaccinated to the WT and recovered from MT (w_2) increased linearly with slope L. The equations of the lines are given by (c) $w_1(t) = ct$ for $t < t^*$ (d) $w_1(t) = w_1(t^*) - L(t - t^*)$ for $t > t^*$ (e) $w_2(t) = L(t - t^*)$ for $> t^*$. (F) Before MT takeover, the dynamic lockdown is adjusted to the WT. As the number of individuals immune to WT grows, social activity increases. When the MT emerges, lockdown measures are reinstated. Subsequently, social activity increases as the population immune to the MT grows. The equations for the lines given by (f) $s(t) = a/\beta_1 x(t)$ for $t < t^*$; (g) $s(t) = a/\beta_2(x(t) + z_1(t) + w_1(t))$ for $> t^*$. Parameters: $N = 10^6$; $a = 0.25$; $d = 0.01$; $\mu = 10^{-6}$; $s_0 = 0.1$; $\beta_1 = \beta_2 = 7.5 \cdot 10^{-7}$; $c = 10,000$; $L = 1500$; $q = 1$.
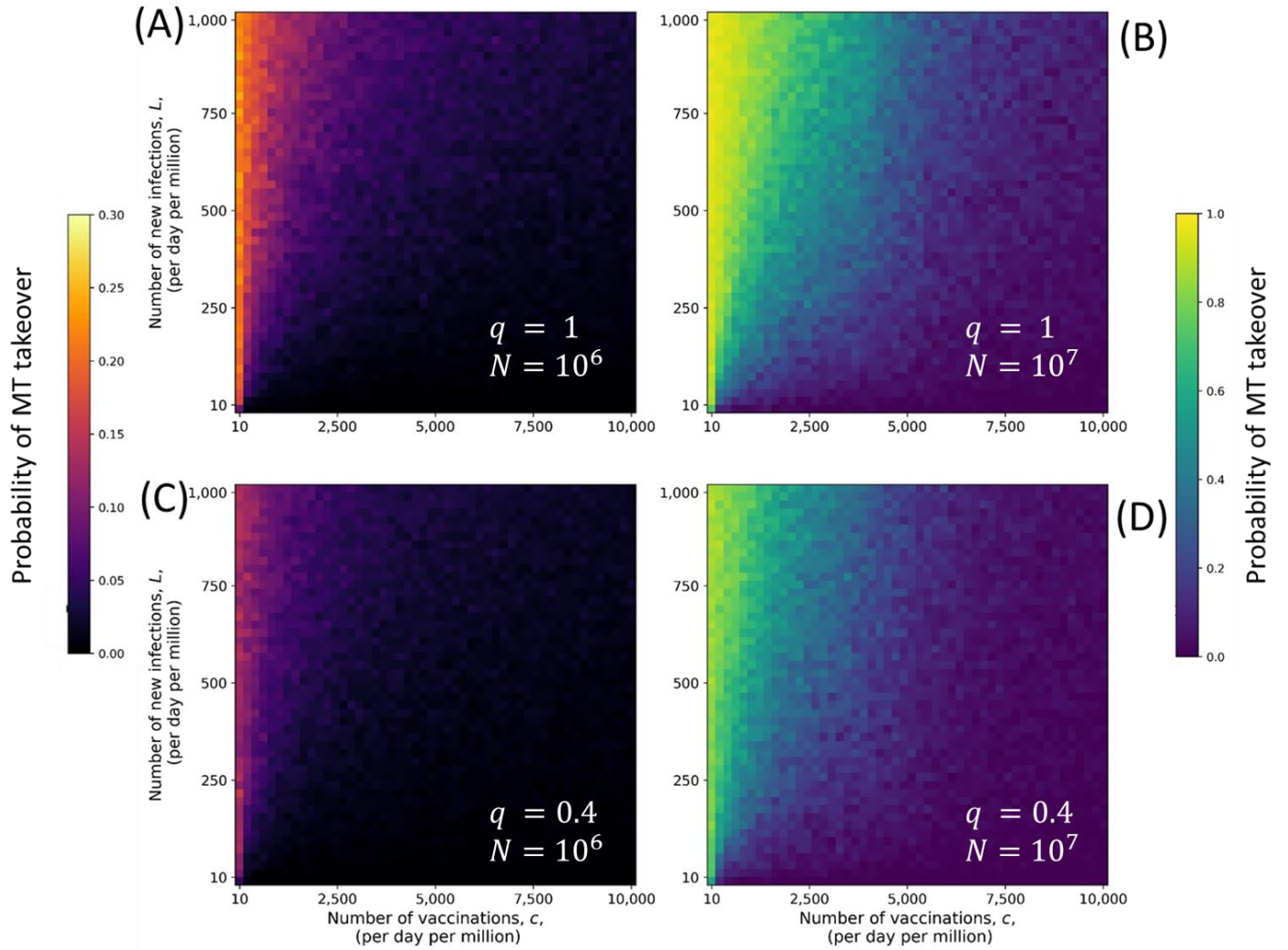
828

829

Figure 4: Probability of emergence of resistance. For each square of the color maps, the proportion of runs (out
of 1000 runs) where the number of individuals infected with the MT strain exceeded the number of individuals
infected with the WT strain is recorded. All simulations are run for a population size of $N = 10^6$, then scaled to
obtain the results shown for $N = 10^7$. Results for color maps (B) and (D) were scaled according to $(1 -
(1-p)^{10})$, where p is the proportion of runs where the MT strain took over. We observe a triangular shape of
(L, c) parameter sets for which the MT strain takes over, indicating that high vaccination rates can be safely
associated with more lenient social distancing measures. On the other hand, very slow vaccination cannot be
compensated by any strength of lockdown. Partial immunity to the MT strain - (C) and (D) - does not affect the
shape of the parameter space where we observe MT takeover, but reduces its probability. Parameters: $a =
0.25; d = 0.01; \mu = 10^{-6}; s_0 = 0.1; \beta_1 = \beta_2 = 7.5 \cdot 10^{-7}$.
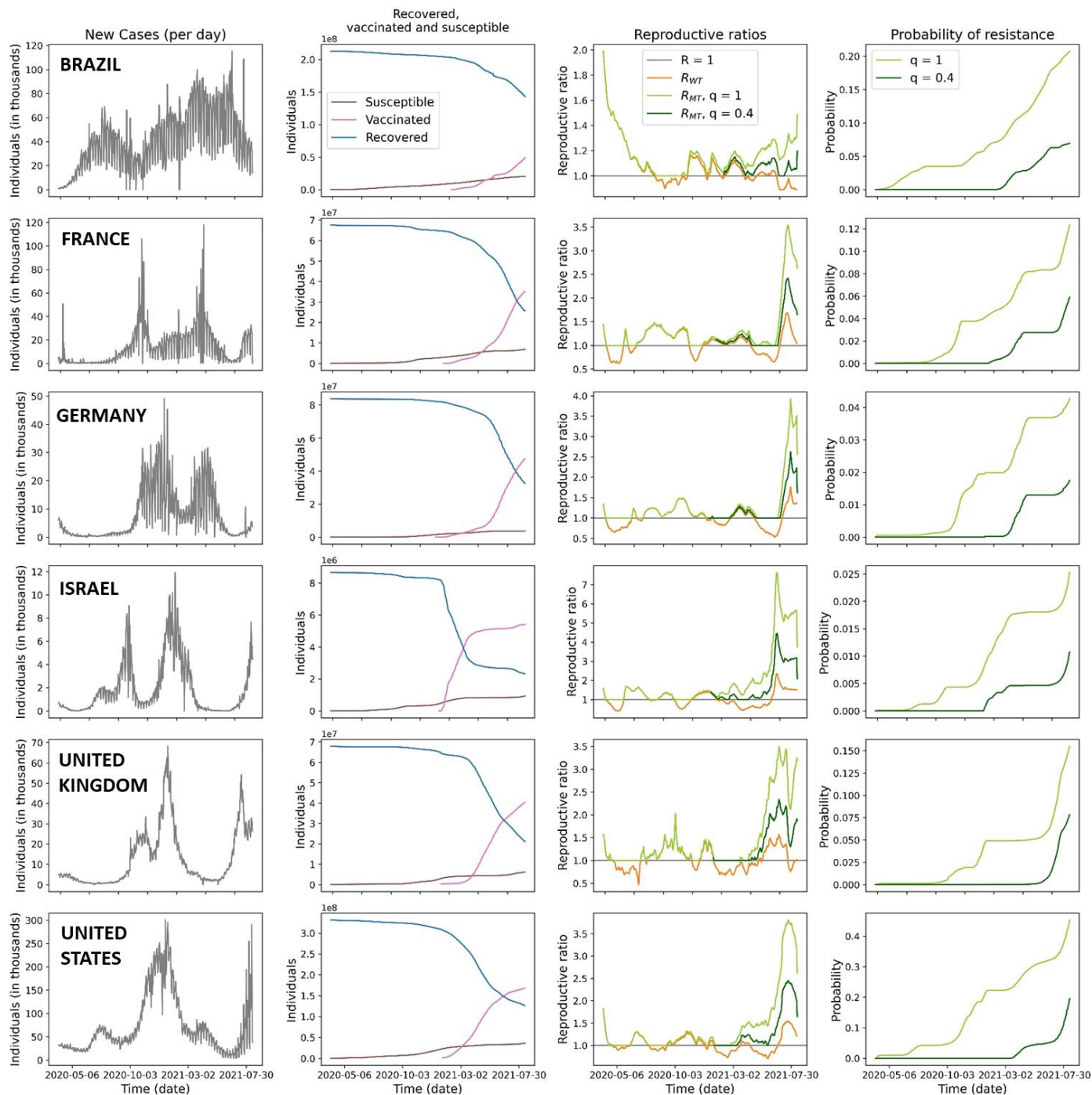
840

841

842

843

844

845

Figure 5: Infection, vaccination data, reproductive ratios and probability of resistance for Brazil, France, Germany, Israel, UK, and US. The total number of new cases per day, number of susceptible, recovered, and vaccinated individuals was downloaded from the *OWID* (Our World In Data) database. We used the *OWID* estimate for the WT reproductive coefficient R_{WT} to calculate the potential MT reproductive coefficient R_{MT} for a full escape mutant, $q = 1$ and a partial escape mutant, $q = 0.4$, (third column). We use Eq. 2 to estimate the probability that an escape mutant would have emerged by time t assuming $\mu = 10^{-7}$ (fourth column).
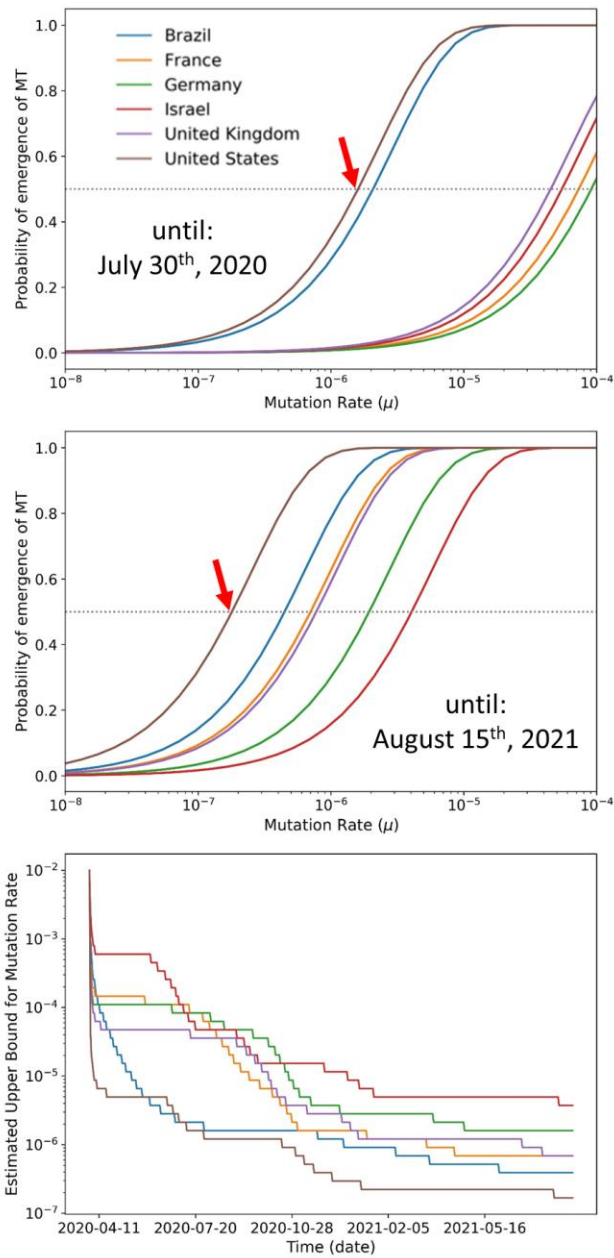
855

Figure 6: Estimating the mutation rate given that no vaccine resistant mutant has taken over. (A) Using Eq. 2, we calculate the probability that a MT strain would have taken over by July 30th, 2020. To this aim, we used the numbers of new infections and immunized individuals (needed to calculate the reproductive coefficient of the MT strain R_{MT} at each time point) from OWID [1]. The probability of MT strain takeover follows a sigmoidal function, where the midpoint is reached for the value of μ where MT strain takeover becomes more probable than not. We consider this value of μ the "upper bound" for the mutation rate. For the US, the estimated upper bound for the mutation rate on July 30th, 2020 would be about 10^{-6} (red arrow). **(B)** Using Eq. 2, we calculate the probability that a MT strain would have taken over by August 15th, 2021. We observe that the curves describing the probability of takeover of the MT strain along mutation rate have shifted left. This is because since July 30th, 2020, additional cases have occurred without a MT strain takeover. Therefore, the upper bound for the mutation rate decreases. For the US, the upper bound for the mutation rate would now be estimated at $2 \cdot 10^{-7}$ (red arrow). **(C)** The midpoint of the function (red arrows shown in (A) and (B)) describing the probability of MT strain takeover decreases in value as more time passes without takeover of an MT strain. We use this value as an upper bound of the mutation rate for our model.